Int. J. Dev. Biol. In Press
https://doi.org/10.1387/ijdb.240222sb

THE INTERNATIONAL JOURNAL OF DEVELOPMENTAL BIOLOGY
www.intjdevbiol.com

Inhibition of COX2 impairs angiogenesis and causes vascular defects in developing zebrafish embryos

LAKSHMI PILLAI, VISHAKHA NESARI, DHANUSH DANES, SURESH BALAKRISHNAN*

Department of Zoology, Faculty of Science, The Maharaja Sayajirao University of Baroda, Vadodara, India

ABSTRACT This study investigated the role of cyclooxygenase-2 (COX2) in angiogenesis during zebrafish embryogenesis by inhibiting COX2 activity with etoricoxib. Liquid chromatography-tandem mass spectrometry (LC-MS/MS) analysis confirmed the successful penetration of etoricoxib into zebrafish embryos, leading to selective inhibition of COX2 without affecting COX1 activity. COX2 inhibition caused a significant reduction in prostaglandin E_2 levels throughout development. Phenotypically, treated embryos exhibited pericardial edema, bradycardia, and defective vascular development, including delays in intersegmental vessel (ISV) sprouting, incomplete dorsal longitudinal anastomotic vessel (DLAV) formation by 48 hpf, and impaired vascular networks by 72 hpf. Confocal imaging and AngioTool analysis revealed reduced vessel length, area and increased lacunarity. Molecular analysis showed significant downregulation of vascular endothelial growth factor A (vegfa), *kdr*, *pi3k* and *akt* transcripts, as well as reduced VEGFA, EP4 and Akt protein levels, disrupting VEGFA-PI3K-Akt signaling. Additionally, reduced expression of *ephrinb* and *prox1* affected arterial and venous identity formation. These results demonstrate that COX2 is essential for proper angiogenesis during zebrafish development, and its inhibition leads to significant vascular defects, underscoring COX2's crucial role in regulating VEGFA-mediated angiogenesis.

KEYWORDS: angiogenesis, COX2 inhibition, prostaglandin E2, vascular development, zebrafish embryos

Introduction

The cardiovascular system is among the earliest to develop in vertebrate embryogenesis, with the heart and blood vessels, including arteries, veins, capillaries, and lymphatic vasculature, forming during the initial stages (Udan *et al*., 2012). These components are crucial for the transport of oxygen, nutrients, and signaling molecules, as well as the removal of metabolic waste products, ensuring tissue homeostasis (Schuermann *et al*., 2014). Advancements in blood vessel biology have highlighted the involvement of blood vessels in pathological conditions like cancer and cardiovascular diseases, leading to new therapeutic strategies targeting the vasculature (Chung *et al*., 2010). This underscores the critical role of blood vessels in maintaining health and combating disease.

Blood vessel formation occurs via two primary mechanisms: vasculogenesis and angiogenesis. Vasculogenesis refers to the de novo formation of vessels from mesodermal precursors, while angiogenesis involves the sprouting and expansion of new vessels from pre-existing ones (Wiens *et al*., 2010). Although vasculogenesis establishes the primary vascular framework, angiogenesis drives the remodeling, growth, and maturation of this network. Angiogenesis plays a pivotal role in physiological processes like reproduction and wound healing, as well as in pathological contexts such as tumor progression (Otrock *et al*., 2007). Given its involvement in both normal and disease states, angiogenesis has become a major focus in developmental biology and therapeutic research.

Zebrafish (*Danio rerio*) have become a preferred model for studying angiogenesis due to their optical transparency, external development, and close genetic similarity to humans. These features enable both *in vivo* imaging and genetic manipulation (Chávez *et al*., 2016). During early development in zebrafish, vasculogenesis forms the major vessels, such as the dorsal aorta (DA) and posterior cardinal vein (PCV), followed by angiogenesis, which drives the sprouting of intersegmental vessels (ISVs) (Isogai *et al*., 2001). ISVs begin sprouting from the DA around 24 hours post-fertilization (hpf), migrating between somites, and establishing connections with the dorsal longitudinal anastomotic vessel (DLAV) at approximately 48 hpf. By the time the embryos reach 72 hpf, the vascular network is fully developed and circulation is active (Childs *et al*., 2002). This entire process is tightly

***Address correspondence to:** Suresh Balakrishnan. Department of Zoology, Faculty of Science, The Maharaja Sayajirao University of Baroda, Vadodara- 390002, India.
E-mail: b.suresh-zoo@msubaroda.ac.in | https://orcid.org/0000-0002-6559-022X

Submitted: 25 October, 2024; Accepted: 23 January, 2025; Published online: 24 March, 2025.

ISSN: Online 1696-3547, Print 0214-6282

regulated by vascular endothelial growth factor A (VEGFA), which binds to its receptor KDR to induce angioblast proliferation and upregulate proliferating cell nuclear antigen (PCNA), a key factor in angiogenesis (Takahashi *et al*., 1995).

While the VEGF signaling pathway is well established in angiogenesis (Liang *et al*., 2001), further research is necessary to elucidate the full spectrum of upstream regulators that modulate this pathway. These regulators are often context-dependent, making it challenging to delineate their precise roles in physiological versus pathological conditions, such as cancer. Thus, although VEGF and its receptors are extensively studied, a comprehensive understanding of their regulation remains an active area of research.

Studies in the past have highlighted cyclooxygenase-2 (COX2) as a potential modulator of angiogenesis (Eckenstaler *et al*., 2022). COX2, traditionally known for its role in prostaglandin synthesis during inflammation (Ricciotti and FitzGerald, 2011), is now recognized for its broader influence on developmental processes. COX2-derived prostaglandins have been implicated in cell proliferation, migration, and differentiation in chick embryos (Verma *et al*., 2021). Moreover, COX2 is essential for proper heart formation in chick embryos (Parmar *et al*., 2022) and photoreceptor development in zebrafish (Li *et al*., 2019), suggesting its critical role in multiple aspects of embryogenesis.

Building on this emerging evidence, we hypothesize that COX2 is a key regulator of angiogenesis during zebrafish development. Specifically, we propose that inhibiting COX2 disrupts normal blood vessel formation, causing defects in the vascular system and delays in its establishment. To test this hypothesis, this study focuses on investigating the impact of COX2 inhibition on the development of intersegmental vessels and the overall vascular network in zebrafish embryos. By exploring the molecular mechanisms through which COX2 influences angiogenesis, our research aims to shed light on its developmental role and assess its potential as a therapeutic target for vascular-related diseases.

Results

Etoricoxib inhibited the activity of COX2 and reduced the PGE_2 production

Zebrafish embryos were exposed to 7 µg/ml etoricoxib added to the E3 medium, and the presence of etoricoxib in the embryos was confirmed using LC-MS/MS analysis. Representative chromatograms are shown in Fig. 1. In the treated group (Fig. 1B), a distinct peak with an m/z value of 359, corresponding to etoricoxib, was observed with a retention time of 2.14 minutes, identical to the peak found in the standard solution (Fig. 1C), as highlighted in red. This peak was absent in the control group (Fig. 1A), where only a peak with an m/z value of 149, representing the matrix, was detected. These results confirm that etoricoxib successfully penetrated the chorion and entered the zebrafish larvae in the treated group, while it was completely absent in the control group.

The dose of 7 µg/ml etoricoxib used in this study was determined based on a dose range study, which identified this concentration as optimal for effectively inhibiting COX2 activity without causing non-specific toxicity. The dose-response curve supporting this selection is shown in Supplementary Fig. 1 for reference.

The activities of COX1 and COX2 were measured at 24, 48, and 72 hpf in both control and treated embryos (Fig. 2). COX1 activity remained unchanged between the control and treated groups

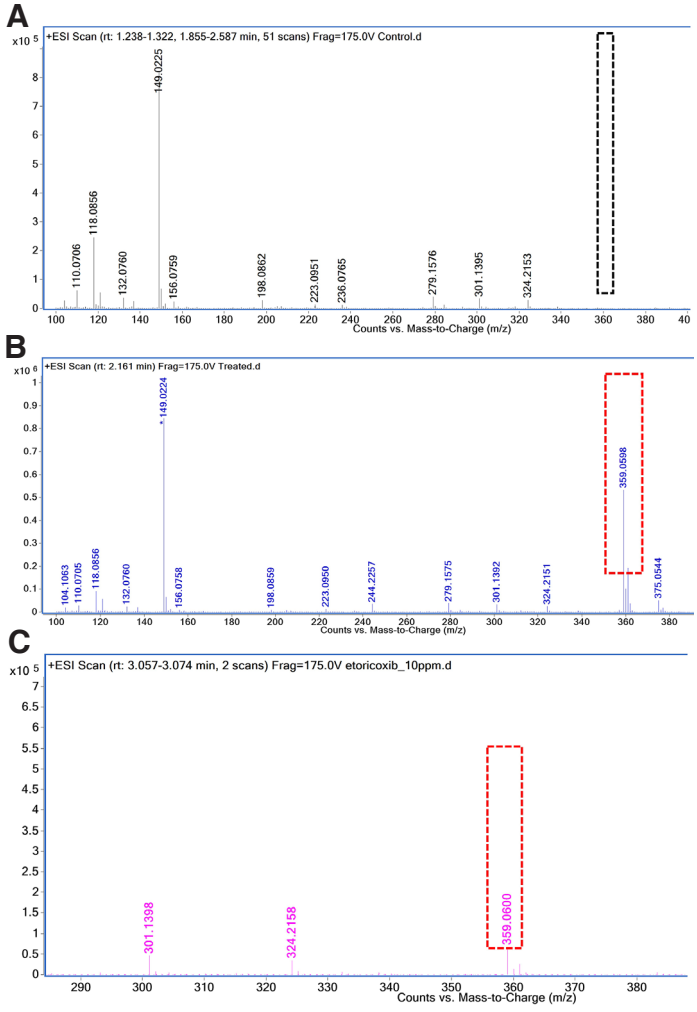

Fig. 1. Representative liquid chromatography-tandem mass spectrometry (LC-MS/MS) profile. (A) Control group. **(B)** Treated group. **(C)** Etoricoxib pure compound (Standard Solution). The etoricoxib fragment of M.W. (359) has been highlighted in a red dotted rectangle. A black dotted rectangle shows the absence of the corresponding peak.

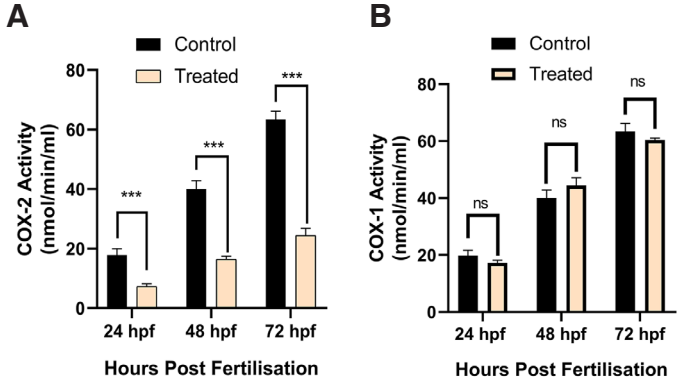

Fig. 2. Cyclooxygenase (COX) enzyme activity levels. (A) COX2 activity. **(B)** COX1 activity in zebrafish embryos of control and treated group at 24, 48 and 72 hpf stages. ***p ≤ 0.001; ns, non-significant; n=3, N=50.

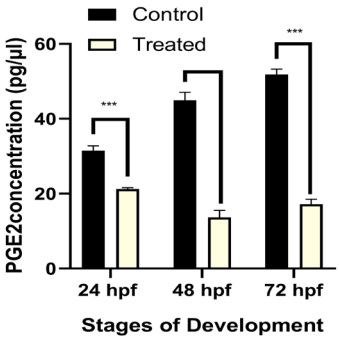

Fig. 3. ProstaglandinE2 (PGE_2) estimation in zebrafish embryos of control and treated group. The assayed stages are 24, 48 and 72 hpf. ***p ≤ 0.001; n=3, N=50.

across all time points, indicating that etoricoxib selectively inhibits COX2 without affecting COX1. Conversely, COX2 activity was significantly inhibited in the treated group at all stages (24, 48, and 72 hpf) compared to the control group, as shown in Fig. 2A. To further support this selectivity, COX1 activity data are presented separately as Fig. 2B.

To validate the biological consequences of COX2 inhibition, prostaglandin E2 (PGE_2) levels were assessed. As shown in Fig. 3, PGE_2 production was significantly reduced in the etoricoxib-treated group across all developmental time points (24, 48, and 72 hpf), confirming that COX2 inhibition directly suppressed PGE_2 synthesis. Importantly, COX1 activity did not compensate for this reduction, as PGE_2 levels remained consistently suppressed in the treated embryos.

The corresponding COX2 activity values are provided in Supplementary Table 1, and the PGE_2 concentrations are detailed in Supplementary Table 2. Taken together, these findings confirm that etoricoxib selectively targets COX2, resulting in a significant reduction in PGE_2 levels during zebrafish embryogenesis without affecting COX1 activity.

The inhibition of COX2 phenotypically disrupted the blood vessel formation

Gross morphological examination of etoricoxib-treated zebrafish embryos at 24, 48, and 72 hpf revealed the presence of pericardial edema (Fig. 4 B,D,F) and bradycardia, a defect absent in the control embryos (Fig. 4 A,C,E). As a result, bradycardia was exhibited by the treated embryos. The heartbeats (beats per minute) have been presented in Supplementary Table 3. Confocal imaging of the fli1:eGFP transgenic zebrafish line, presented in Fig. 5 A-L, along with corresponding quantifications of blood vessel length, blood vessel area, and lacunarity (Fig. 6), indicate that COX2 inhibition significantly impaired angiogenic progression.

Blood vessel length and area, which reflect the spatial distribution of intersegmental vessels (ISVs) in the trunk region, were notably reduced in the treated embryos. Lacunarity, representing the gaps or empty spaces within the angiogenic network, was increased, suggesting a disrupted vascular architecture (Danes *et al*., 2024). At 24 hpf, angiogenic sprouts were readily observable in control embryos (Fig. 5A), whereas the treated embryos (Fig. 5B) displayed a marked reduction in sprout formation. By 48 hpf, control embryos (Fig. 5C) showed well-developed sprouts that migrated and fused with the dorsal longitudinal anastomotic vessel (DLAV), as indicated by yellow annotations. In contrast, although treated embryos (Fig. 5D) exhibited some migration of angiogenic sprouts, forming a characteristic "T" shape, they failed to anastomose and complete DLAV formation (Gore *et al*., 2012).

By 72 hpf, control larvae (Fig. 5E) demonstrated advanced angiogenesis, with notable hyperbranching of arteries, the formation of the parachordal vessel (PAV) and primordial vertebral artery (VTA), as well as the clear specification of arterial and venous identities. In treated larvae (Fig. 5F), while the fusion of sprouts to form DLAV was evident, key features such as hyperbranching, PAV, and VTA formation were absent, indicating a significant delay or impairment in angiogenic development (Ribatti and Crivellato, 2012).

Quantitative analysis using AngioTool further supported these observations. The etoricoxib-treated embryos exhibited a reduction in blood vessel length and area, accompanied by an increase in lacunarity, at all three developmental stages. These findings align with the morphological defects observed in the confocal images (Fig. 4 A-F), where reduced angiogenic sprouting and diminished blood vessel size were prominent. The impaired angiogenic progression ultimately led to a pericardial edema-like phenotype, as evident in Fig. 5 A-F. These results confirm that COX2 inhibition severely disrupts angiogenesis, manifesting in both morphological and functional vascular deficiencies in zebrafish embryos. The numerical values of quantifications of blood vessel

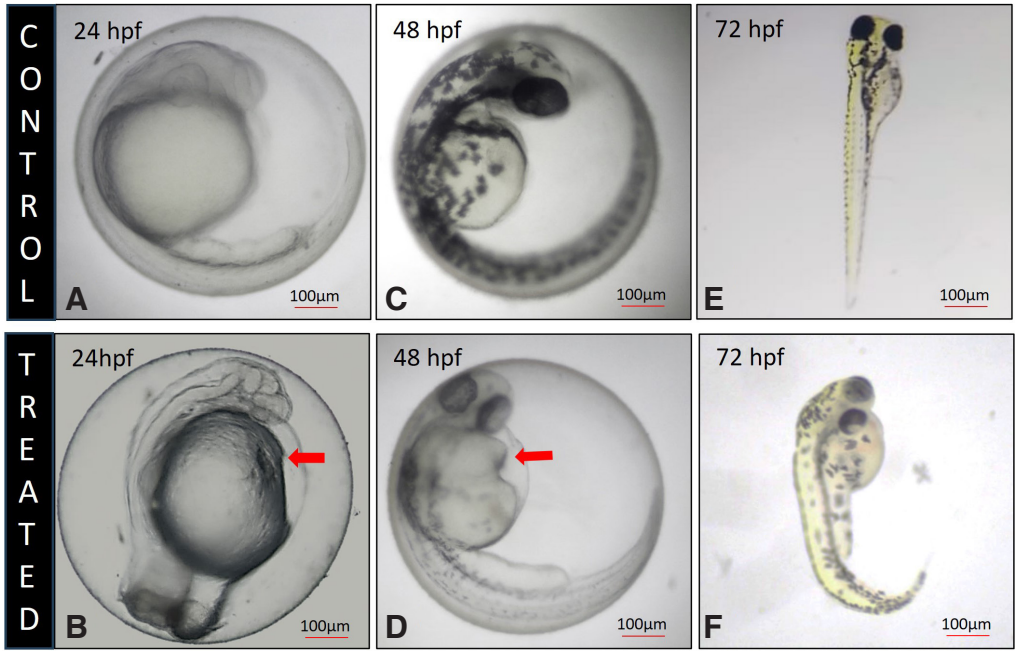

Fig. 4. Morphology of 24, 48 and 72 hpf zebrafish larva. (A,C,E) Control zebrafish larva, displaying heart. **(B,D,F)** Etoricoxib treated zebrafish larva, showing pericardial edema in the heart (red arrow).

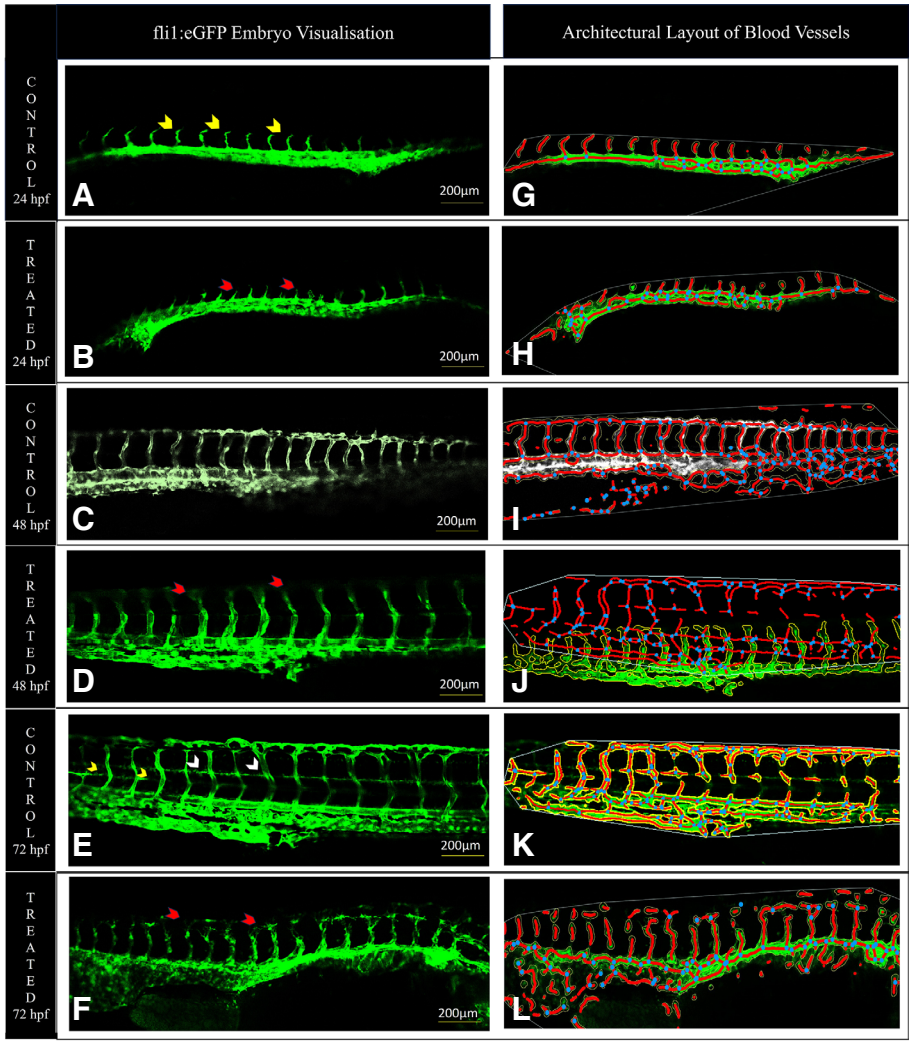

Fig. 5. Confocal images of the fli1: eGFP transgenic line. (A) Control 24 hpf embryos (yellow arrowhead indicates angiogenic sprouts). **(B)** Treated 24 hpf embryos (red arrowhead indicates shrunken angiogenic sprouts). **(C)** Control 48 hpf; yellow arrowhead indicates DLAV (dorsal longitudinal anastomotic vessel). **(D)** Treated 48 hpf embryos (yellow arrowhead indicates the extension of angiogenic sprouts). **(E)** Control 72 hpf larvae (white arrowhead showing PAV (parachordal vessel) and red arrowhead showing VTA (primordial vertebral artery). **(F)** Treated 72 hpf larvae (red arrowhead indicates the delayed established DLAVs). 2nd column **(G-L)**: Architectural layout of the vascular network processed on AngioTool software.

length, blood vessel area, and lacunarity are represented in Supplementary Tables 4,5,6.

The inhibition of COX2 activity downregulated the expression of angiogenesis markers

Key angiogenic markers and associated signaling molecules were assessed for differential gene expression in zebrafish embryos. The gene and protein expression study was carried out using wildtype embryos instead of fli1:eGFP since the transgenic line can cause inaccurate quantification of genes as they are subjected to genetic modification. Transcript levels of *vegfa, kdr, ep4, pi3k*, and *akt* were significantly downregulated at 24, 48, and 72 hpf, while *caspase3* expression was markedly elevated in the etoricoxib-treated group. In addition, the expression of *pcna* at 24 hpf, *cdh5* at 48 hpf, and *ephrinb*, and *prox1* at 72 hpf was also reduced in treated embryos compared to controls. 18S rRNA was used as the endogenous control for normalization, and the relative fold changes in expression are illustrated in Fig. 7.

Protein expression levels for *VEGFA*, EP4, and Akt followed a similar trend as observed for their transcript levels. At 48 and 72 hpf, these proteins were significantly downregulated in the treated group, whereas at 24 hpf, the reduction in protein expression was not statistically significant (Fig. 8 A-C). The levels of cleaved Caspase-3 were markedly elevated in all treated groups, indicating increased cell death. GAPDH was used as the endogenous control for normalizing protein expression. The quantified band intensities corresponding to protein levels are presented in Supplementary Table 6, and representative Western blot images are shown in Fig. 8D.

The whole-mount localization experiment revealed the spatial distribution of VEGFA. In the control group (Fig. 9A), VEGFA expression was predominantly observed in the intersegmental vessels, indicated by red arrowheads.

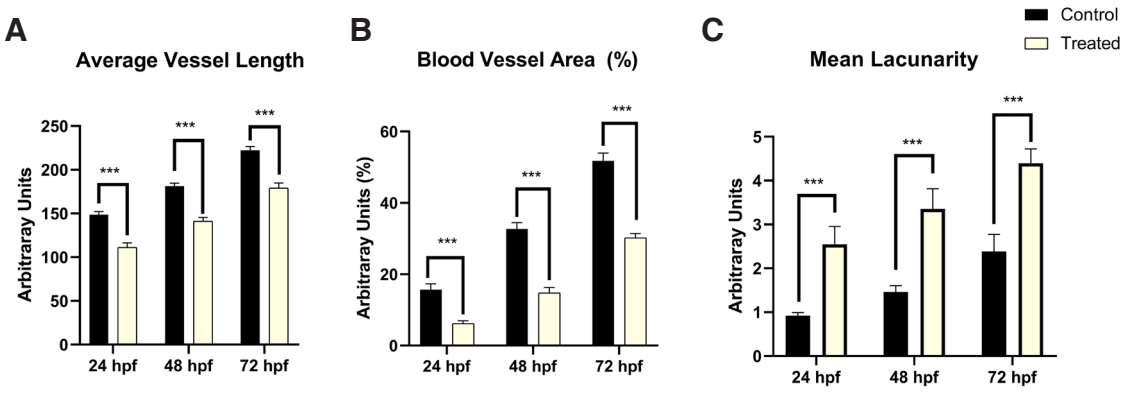

Fig. 6. Analysis of vasculature of fli1:eGFP embryos using AngioTool software. The stages of assessment are 24, 48 and 72 hpf. **(A)** Average blood vessel length. **(B)** Blood vessel area (%). **(C)** Mean lacunarity. ***p ≤ 0.001; n=3, N=50.

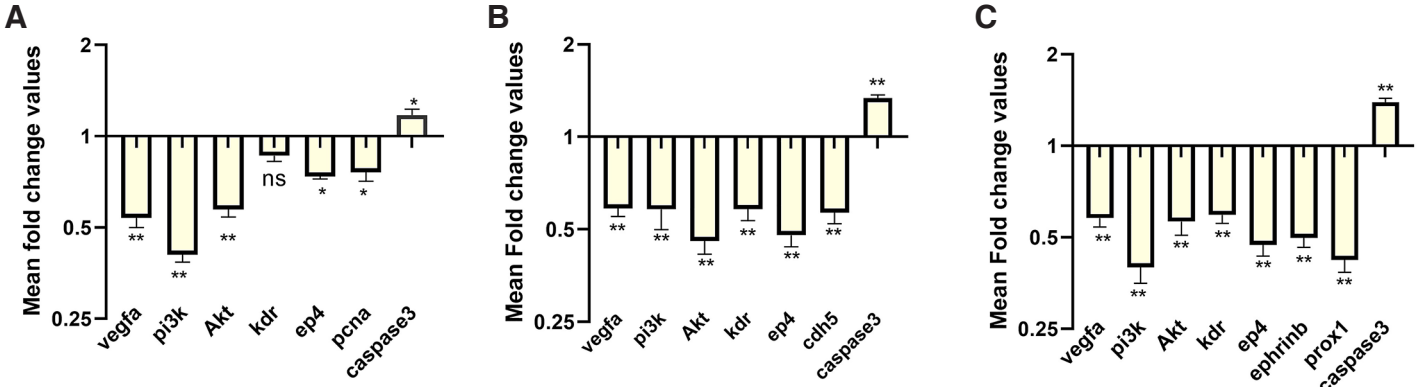

Fig. 7. Mean fold change in the expression of the genes involved during angiogenesis in etoricoxib treated zebrafish embryos. (A) 24 hpf, **(B)** 48 hpf and **(C)** 72 hpf stages. The fold change value for the control group was kept as 1. ns, not significant, *p ≤ 0.1 and **p ≤ 0.01; n = 3; N=75.

This strong expression reflects its pivotal role in promoting angiogenesis and vascular development by mediating endothelial cell proliferation and migration during vessel formation. In contrast, the treated larvae (Fig. 9D) exhibited markedly reduced fluorescence intensity, indicative of diminished VEGFA expression. Although VEGFA expression remained detectable in the treated specimens, the significant reduction in fluorescence intensity suggests that etoricoxib treatment disrupts VEGFA-mediated signaling pathways.

These findings indicate that the inhibition of COX2 activity led to reduced expression of key molecules involved in angiogenesis, blood vessel proliferation, and arterial identity, particularly at later stages of zebrafish development. The downregulation of both gene and protein expression highlights the role of COX2 in regulating these critical pathways during vascular development.

Discussion

Cyclooxygenases are key enzymes in the prostaglandin synthesis pathway, catalyzing the conversion of arachidonic acid into various prostanoids, including prostaglandin E2 (PGE_2). These enzymes exist as two isoforms: COX1 and COX2. Historically, COX1 has been regarded as essential for producing prostaglandins critical for early embryonic processes in zebrafish (Cha *et al*., 2006b). Consistent with this view, Cha *et al*.,2005) demonstrated that COX1 plays a pivotal role in vascular tube formation during zebrafish development. In contrast, COX2 has been predominantly associated with inflammatory responses and was not initially linked to developmental functions (Ricciotti and Fitzgerald, 2011). However, the use of COX2-selective inhibitors during pregnancy has been implicated in fetal ductus arteriosus closure (Antonucci

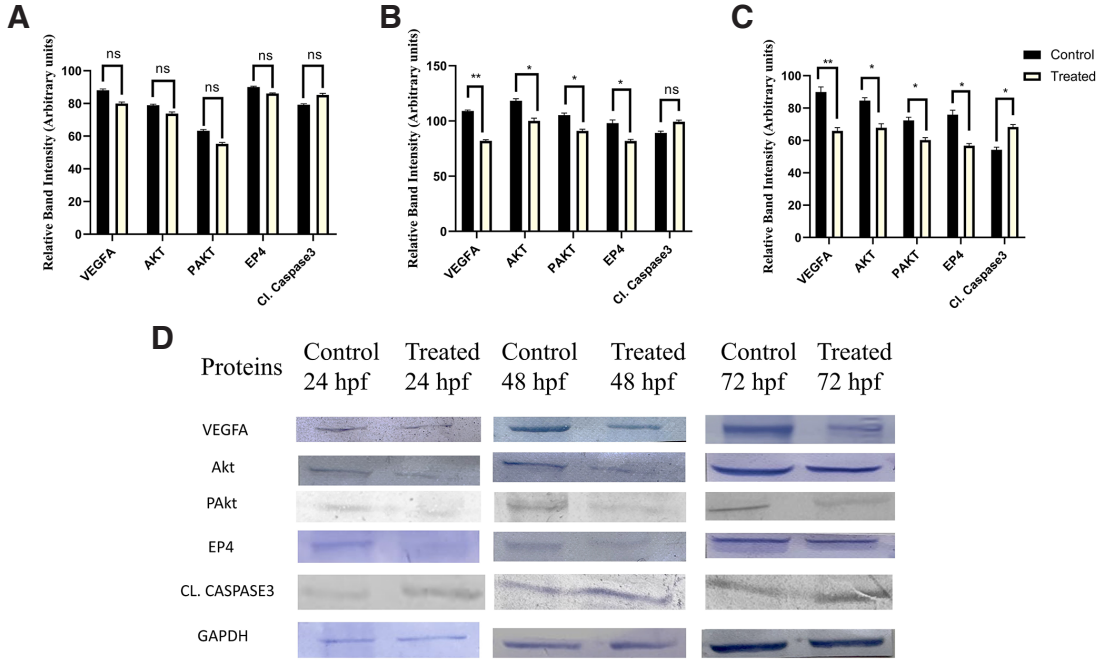

Fig. 8. Protein Expression Analysis. (A-C) Densitometric analysis of proteins involved during angiogenesis in control and etoricoxib treated zebrafish embryos. The stages of assessment were **(A)** 24 hpf, **(B)** 48 hpf and **(C)** 72 hpf. ns, not significant, *p ≤ 0.1 and **p≤0.01. n = 3; N=75. **(D)** Representative Western blot images of the corresponding stages.

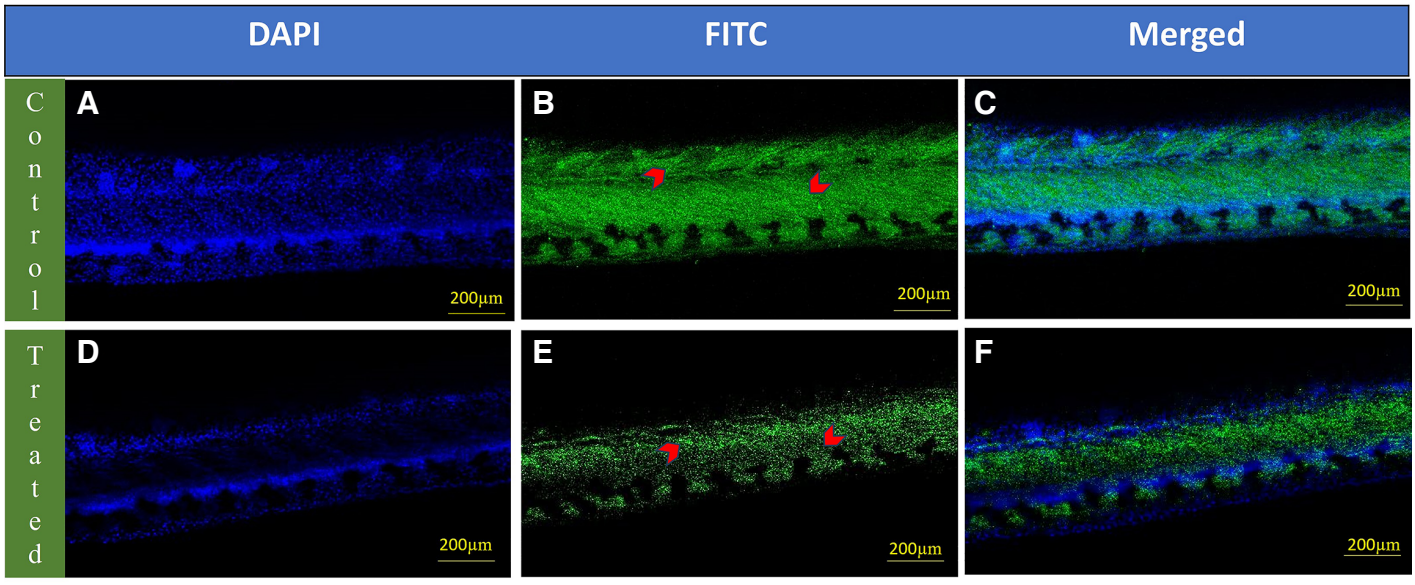

Fig. 9. Whole-mount localization of vascular endothelial growth factor A (VEGFA) in the intersegmental vessels of 72 hpf zebrafish larvae. The upper panel **(A-C)** shows images of control zebrafish larvae: **(A)** Nuclei stained with DAPI (blue), **(B)** VEGFA immunolabeling visualized using FITC (green), with red arrowheads indicating VEGFA expression in the intersegmental blood vessels and **(C)** merged image combining DAPI and VEGFA signals. The lower panel **(D–F)** shows images of etoricoxib-treated zebrafish larvae: **(D)** Nuclei stained with DAPI (blue), **(E)** VEGFA immunolabeling visualized using FITC (green), with red arrowheads indicating VEGFA expression in the intersegmental blood vessels and **(F)** merged image combining DAPI and VEGFA signals.

et al., 2012; Cha *et al*., 2006a), suggesting an unanticipated developmental role for COX2. Additionally, the localization of COX2 in the pharyngeal arches of 5-day-old zebrafish larvae further supports this possibility (Grosser *et al*., 2002). These findings necessitate a reevaluation of COX2's role beyond inflammation, with a focus on its potential developmental functions.

Emerging evidence has highlighted COX2's involvement in key developmental processes. For instance, COX2-derived prostacyclin (PGI_2) has been shown to play a crucial role in early mouse embryo development *in vitro* (Pakrasi and Jain, 2007). Similarly, COX2 has been implicated in the migration of cranial neural crest cells in chick embryos (Parmar *et al*., 2021). In zebrafish, exposure to the COX2 inhibitor celecoxib resulted in cardiac defects, such as bradycardia and underdeveloped hearts (Xu *et al*., 2011). These findings suggest that COX2's role in development cannot be compensated by COX1, underscoring its unique and essential function. Notably, COX2 has been localized in zebrafish pharyngeal arches during development, suggesting a specific role in angiogenesis (Pini *et al*., 2005). Furthermore, studies have linked COX2 to *vegfa* signaling during tissue regeneration in other vertebrates, reinforcing its involvement in vascular development (Ugwuagbo *et al*., 2019). Recent insights have also indicated that COX2 metabolites, including hemiketal E2, enhance VEGFR2 activation through a 5-lipoxygenase/COX2 crossover pathway, amplifying endothelial tubulogenesis and promoting angiogenesis (Nakashima *et al*., 2023). Given these findings, the current study aimed to explore COX2's specific role in zebrafish angiogenesis.

The results of this study, confirmed by LC-MS/MS analysis, demonstrated that etoricoxib, a potent COX2 inhibitor, successfully penetrated zebrafish embryos and caused notable phenotypic and molecular changes. COX activity assays revealed that etoricoxib selectively inhibited COX2 without affecting COX1 activity, leading to a significant reduction in PGE_2 production throughout development. This reduction highlighted COX2's critical role in PGE_2 synthesis, a function that COX1 was unable to compensate. These findings align with reports in vertebrates where selective COX2 inhibitors significantly reduced PGE_2 production, a critical regulator of vascular development (Ricciotti and Fitzgerald, 2011).

Phenotypically, embryos treated with etoricoxib exhibited pericardial edema and bradycardia, commonly associated with defective blood vessel development (Heideman *et al*., 2005). Confocal imaging of fli1: eGFP transgenic embryos revealed significant delays in angiogenic sprouting at 24 hours post-fertilization (hpf), incomplete formation of the dorsal longitudinal anastomotic vessel (DLAV) by 48 hpf, and defective vascular network formation by 72 hpf. Quantitative analysis using AngioTool confirmed a reduction in vessel length and area, alongside increased lacunarity in treated embryos, further underscoring the impaired angiogenesis. These phenotypes are consistent with observations of impaired vascularization following COX2 inhibition in vertebrate models, including zebrafish and mice (Xu *et al*., 2011; Ugwuagbo *et al*., 2019).

Angiogenesis is initiated by vascular endothelial growth factor A (*vegfa*), which binds to its receptor KDR on endothelial cells, promoting the elongation and proliferation of vascular sprouts through the upregulation of proliferating cell nuclear antigen (*pcna*) at 24 hpf (Karar and Maity, 2011). This process is mediated by the PI3K-Akt pathway, which is critical for *vegfa* signaling. PGE_2, acting through the EP4 receptor, further amplifies this pathway by stimulating *vegfa* production through PI3K-Akt activation (Iwasaki *et al*., 2019).

Following vascular sprouting, intersegmental vessels (ISVs) undergo lumenization, migrating as multicellular sprouts from the primary vessel while maintaining a continuously connected lumen

(Nasevicius *et al*., 2000). By 48 hpf, the ISVs connect to form the dorsal longitudinal anastomotic vessel (DLAV), establishing active circulation from the brain to the tail regions. The *vegfa*-Akt interaction also regulates cadherin-5 (*cdh5*), which plays a pivotal role in guiding vascular sprouts and ensuring proper lumen formation (Lammert and Axnick, 2012).

In this study, COX2 inhibition led to a significant reduction in *vegfa*, *kdr*, *ep4*, *pi3k*, and *akt* transcript levels, accompanied by a corresponding decrease in VEGFA, EP4, Akt, and phosphorylated Akt (PAkt) protein levels. At 48 and 72 hpf, protein levels of VEGFA, EP4, and Akt were significantly downregulated in the treated group, while at 24 hpf, the reduction was not statistically significant. This was evidenced by incomplete ISV formation at 24 and 48 hpf. Whole-mount localization experiments revealed that in the control group, VEGFA expression was predominantly observed in the ISVs, demonstrating its established role in promoting angiogenesis and vascular network formation. In contrast, the treated larvae exhibited a marked reduction in VEGFA expression intensity, impairing vascular sprouting and lumen formation. These findings highlight the critical interplay between COX2 and the VEGFA-PI3K-Akt axis, demonstrating how COX2 inhibition disrupts *vegfa* signaling, ultimately impairing angiogenic processes in zebrafish embryos.

By 72 hpf, arterial and venous identities are established, marked by the expression of *ephrinb* and *prox1*, alongside the hyperbranching of vessels, which is crucial for normal vascular development (Kazenwadel and Harvey, 2016). The upregulation of *caspase3* and Cleaved Caspase3 protein in the treated group suggests that cell death predominates over proliferation. This study found that COX2 inhibition disrupted these processes, with diminished expression of *ephrinb* and *prox1* in treated embryos, alongside downregulation of *vegfa*, *pi3k*, and *akt*. These transcriptional changes were reflected at the protein level, resulting in delayed formation of the venous thoracic artery (VTA) and parachordal vessel (PAV) and an overall defective vascular network. The observed disruption of arterial and venous identities aligns with studies in COX2 knockout models that show vascular malformations and incomplete vessel differentiation (Pini *et al*., 2005). These molecular and phenotypic abnormalities underscore COX2's critical role in mediating VEGFA-PI3K-Akt signaling during zebrafish angiogenesis.

In summary, this study demonstrates the indispensable role of COX2 in zebrafish vascular development, particularly in regulating angiogenesis. COX2 inhibition disrupts key signaling pathways that drive blood vessel formation, leading to significant vascular defects. These findings carry broader implications for understanding the risks associated with NSAID use during pregnancy, where COX2 inhibition could contribute to congenital vascular abnormalities. Future research could explore therapeutic approaches, such as COX2-targeted supplementation, to mitigate these developmental effects, offering potential strategies for vascular regeneration.

Material and Methods

Zebrafish maintenance and egg procurement

The zebrafish (*Danio rerio*) used in this study were maintained in compliance with the Committee for Control and Supervision of Experiments on Animals (CCSEA) guidelines at the Department of Zoology, The Maharaja Sayajirao University of Baroda, Vadodara, India (CCSEA Registration No. 827/G.O./Re/S/04/CPCSEA). Adult wild-type zebrafish were procured from a licensed supplier, Oscar Aquarium, located in Vadodara, India. Transgenic zebrafish embryos (fli1:eGFP), used for confocal imaging, were kindly provided by Dr. Chinamoy Patra from the Agharkar Research Institute, Pune. The zebrafish were housed in dechlorinated water with a pH maintained between 7.0 and 7.4, under controlled conditions of 28 ± 2°C and a 12-hour light/12-hour dark photoperiod. For breeding, adult zebrafish were placed in a spawning tank at a male-to-female ratio of 1:2. Eggs were collected within 1.5 hours post-spawning and rinsed with deionized water to remove debris, following the protocol described by Meyers (Meyers, 2018). The collected embryos were transferred to E3 medium for further incubation and developmental studies. The experimental design included two groups: control embryos maintained in E3 media and treated embryos maintained in E3 media containing 7 µg/ml of etoricoxib. Etoricoxib is a selective COX-2 inhibitor widely used to manage symptoms of autoimmune disorders (Martina *et al*., 2005). Technical grade etoricoxib, generously provided by Sun Pharma Advanced Research Company, Vadodara, India, was used for this study. The dose of 7 µg/ml was determined based on a dose range study to ensure effective inhibition of COX2 activity while minimizing off-target effects. Further details of the dose-response study are emphasized in the results section. All experimental protocols were approved by the Institutional Animal Ethics Committee (Approval No. MSU-Z/IAEC04/06-2021) and adhered to institutional and national guidelines for the ethical treatment of laboratory animals.

LC-MS/MS analysis

Liquid chromatography-tandem mass spectrometry (LC-MS/MS) was performed to detect etoricoxib in treated zebrafish larval homogenates. Fifty zebrafish larvae at 72 hpf were collected from both control and treated groups, homogenized in methanol, and centrifuged at 12,000 rpm for 7 minutes at 4°C (Pillai *et al*., 2024). The supernatant was collected, filtered, and used as the experimental sample. A 5 µl aliquot of each sample, along with a standard solution of etoricoxib, was injected into the system at a flow rate of 100 µl/min. The initial separation was performed using a C-18 column (250 mm x 4.6 mm, 5 µm particle size) from Agilent Technologies (USA), with acetonitrile:water (70:30) as the mobile phase. The samples were subsequently analyzed using an Agilent mass spectrometer coupled to the Agilent L.C. system (Agilent Technologies, USA). Positive ionization mode was employed, with instrument parameters set to a gas temperature of 320°C, ion spray voltage of 3000 V, and sheath gas pressure of 35 psig. Data acquisition and analysis were carried out using MassHunter acquisition software B.08.00 (Agilent Technologies, USA).

COX activity assay

To assess cyclooxygenase (COX) activity, zebrafish embryos were collected at 24 hpf, 48 hpf, and 72 hpf from both control and treated groups. The embryos were immediately placed in a pre-chilled buffer (0.1 M Tris-HCl, pH 7.8, 1 mM EDTA) for subsequent analysis of COX1 and COX2 activity. The assay was conducted following the manufacturer's instructions (Cayman Chemicals, Item No. 760151, USA). For each sample, embryos

were homogenized in the buffer and centrifuged at 8000g for 20 minutes at 4°C. The supernatant was carefully collected for further analysis. Background wells (with inactivated supernatant samples), standard wells, sample wells (containing 40 µl of supernatant), and inhibitor wells (with selective COX1 inhibitor SC-560 or COX2 inhibitor DuP-697) were prepared. Assay buffer, heme, and the respective COX solution were added to each well, followed by a 10-minute incubation at room temperature. After incubation, 20 µl of the colorimetric substrate was added to initiate the reaction. Absorbance was measured at 590 nm, detecting the oxidation of N,N,N',N'-tetramethyl-p-phenylenediamine (TMPD), which correlates with the peroxidase activity of COX enzymes. The specific activity of COX was calculated by normalizing the results to the total protein content of each sample. Statistical significance between the control and treated groups was determined using an unpaired t-test, performed with GraphPad Prism (GraphPad Software, USA). Data were expressed as mean ± standard error, and p-values ≤ 0.05 were considered statistically significant.

ProstaglandinE2 (PGE_2) concentration assay

Prostaglandin levels in zebrafish embryos at 24, 48, and 72 hpf were measured using a sandwich ELISA kit, following the manufacturer's guidelines (RnD Systems, Item No. KGE004B, USA). Fifty embryos from each group were collected and homogenized in pre-chilled buffer (0.1 M Tris-HCl, pH 7.8, 1 mM EDTA), then centrifuged at 2000g for 15 minutes at 4°C (Thermo Fisher Scientific, USA). The resulting supernatant was collected, and absorbance was measured at 590 nm using a Bio-Rad microplate reader (Bio-Rad Laboratories, USA). The experiment was repeated in triplicate for accuracy. Statistical analysis of the data was performed using an unpaired t-test in GraphPad Prism (GraphPad Software, USA), with results presented as mean ± standard error, and a significance threshold set at p ≤ 0.05.

Imaging of embryos

To visualize the morphological abnormalities resulting from etoricoxib exposure, live embryos were examined under a light microscope (Magnus, New Delhi, India). Photographs of the embryos were then taken using a camera (Catalyst Biotech, Panvel, India) mounted on the microscope. Confocal imaging of the fli1: eGFP transgenic line carried out using an LSM 710 Confocal Microscope (Carl Zeiss Microscopy, Oberkochen, Germany).

Vascular network analysis using AngioTool

Confocal images of transgenic zebrafish embryos (fli1: eGFP) at 24, 48, and 72 hpf were captured using a confocal microscope (Leica TCS SP8, Leica Microsystems, Germany). The fli1:egfp line was created by expressing EGFP driven by the promoter for fli1. The gene fli1 is an endothelial cell marker and the transgenic line (fli1: eGFP) is particularly used for visualizing the vasculature (Cha and Weinstein, 2007). The images were analyzed using AngioTool software (Version 0.6a, National Cancer Institute, USA) to quantify morphological and geometric parameters of the vascular network, including vessel area, total vessel length, and lacunarity. Statistical analysis was conducted using Student's t-test, with a significance level set at 95% (p ≤ 0.05) to compare differences between control and treated groups. All data are presented as mean ± standard error.

qRT-PCR analysis

Total RNA was extracted from control and treated groups of zebrafish embryos at 24, 48, and 72 hpf using TRIzol reagent (Applied Biosystems, USA), following the manufacturer's protocol. RNA concentration was quantified using a fluorescence-based Qubit assay (Thermo Fisher Scientific, USA). For cDNA synthesis, 1 µg of RNA from each sample was reverse-transcribed using a one-step cDNA synthesis kit (Thermo Fisher Scientific, Item No. 4368814, USA), according to the manufacturer's instructions. Quantitative real-time PCR (qRT-PCR) was performed using the synthesized cDNA, specific primers, and SYBR Green master mix (Bio-Rad, USA) on a LightCycler 96 system (Roche, Switzerland). The PCR protocol included an initial denaturation step at 95°C, followed by 32 cycles of denaturation at 95°C for 10 seconds, annealing at 60°C for 30 seconds, and extension at 72°C for 20 seconds. 18S rRNA was used as the endogenous control to normalize gene expression levels. Relative gene expression was calculated using the $2^{-\Delta\Delta Cq}$ method, based on Livak and Schmittgen (2001). Primer sequences for the target genes are listed in Table 1.

Western blot analysis

Protein expression in zebrafish embryos at 24, 48, and 72 hpf was assessed using SDS-PAGE followed by Western blot analysis. Embryonic lysates were prepared by homogenizing the embryos in lysis buffer (25 mM Tris-Cl, pH 7.2, 140 mM NaCl, and 1× protease inhibitor cocktail; Sigma-Aldrich, USA). The protein samples were then resolved on a 4% stacking and 12% resolving polyacrylamide gel using an electrophoresis system (Bio-Rad, USA). After electrophoresis, the separated proteins were transferred to a polyvinylidene difluoride (PVDF) membrane (Millipore, USA) using a semi-dry transfer system (Bio-Rad, USA). The membrane was blocked and incubated overnight at 4°C with primary antibodies specific to the proteins of interest. Following primary antibody incubation, the membrane was incubated with biotinylated secondary antibodies (Sigma-Aldrich, USA) for 2 hours at

TABLE 1

PRIMER SEQUENCES OF GENES OBTAINED FROM THE NCBI DATABASE FOR QPCR

Genes	Primer	Accession number
vegfa	Fwd: CATCGAAGGCCTGGCTTAGC Rev: CAGACTGAGCGAGAAGCTGA	AY178799
kdr	Fwd: AGAGGAACACCCCACTCTGT Rev: GTCCAGCACAATGCCTGTTG	U82231
ep4	Fwd: GCTGCGGGAGAACAGAAGTA Rev: CTTGGAGGCTTCCTGAGGTC	NM_131404
ephrinb	Fwd: CGCCTCTGCGATTCGTTTTT Rev: TGGCGCCTTTAACACCTCAT	NR_030067.1
pcna	Fwd: AGTGACGGGTTCGACTCCTA Rev: AGGCGTCAGCATTGTCTTCA	NM_131404
prox1	Fwd: TGTGCCTCTCACAATCCCTG Rev: CCTCTCAGCTCCCAAGAACC	JX765811
cdh5	Fwd: AAGAAGCTGACACCTCTCGC Rev: AATTGCGCGTTATCTTGCCC	NR_20512
pi3k	Fwd: GCGAATACTGAAAGGCAGCG Rev: TACAGTCACTGCCGACACAC	NM_67874
akt	Fwd: GACACCTCTCGCCTACAAGC Rev: ATCTTCTTCGTGGTGGACGG	NM_00796
18SrRNA	Fwd: CCTGTGCCGTGTTATGGGAA Rev: TTGGGTCATCAATGGGCAGG	NR_003278
caspase3	Fwd: CCTGTGTTAGTAGGCCCGTA Rev: TTGGGTGTGCATGCTAGAAT	NR_030057

TABLE 2

LIST OF ANTIBODIES USED FOR WESTERN BLOT

Name	Catalogue No.	Manufacturer	Concentration
VEGFA	MAA143H	Sigma-Aldrich, USA	0.5*µ*g/ml
Akt	SAB4500797	Sigma-Aldrich, USA	0.5*µ*g/ml
EP4	SAB1411142	Sigma-Aldrich, USA	0.1*µ*g/ml
GAPDH	CAB932	Cloud-Clone, USA	0.1*µ*g/ml
Anti-Mouse IgG-Biotin	B7401	Sigma-Aldrich, USA	0.5*µ*g/ml
Anti-Rabbit IgG-Biotin	B7389	Sigma-Aldrich, USA	0.5*µ*g/ml
Streptavidin-ALP-Conjugate	11089161001	Sigma-Aldrich, USA	0.5*µ*g/ml
PAkt	44-621G	Thermo Fisher, USA	0.5*µ*g/ml
Cleaved CASPASE3	PA5-114687	Thermo Fisher, USA	0.5*µ*g/ml
FITC – Anti Mouse IgG	F0257	Sigma-Aldrich, USA	0.5*µ*g/ml

room temperature. Subsequently, alkaline phosphatase (ALP)-conjugated streptavidin was added to the membrane, followed by the application of a chromogenic substrate for ALP detection (Thermo Fisher Scientific, USA). The list of primary and secondary antibodies used is provided in Table 2.

Whole mount localisation

Embryos at 72 hpf were collected and fixed overnight in 4% paraformaldehyde at 4°C. Following fixation, the embryos were rinsed with PBS and subjected to antigen retrieval by incubation in a retrieval solution for 20 minutes at 70°C. After cooling to room temperature, the embryos were incubated in a blocking solution to prevent nonspecific binding, followed by overnight incubation at 4°C with the primary anti-VEGFA antibody (Sigma-Aldrich, USA). The next day, a FITC-conjugated secondary antibody (Sigma-Aldrich, USA) was applied and incubated for 1 hour at room temperature. The manufacturer details of the antibodies are presented in Table 2. The labeled embryos were visualized using an LSM 710 Confocal Microscope (Carl Zeiss Microscopy, Oberkochen, Germany). DAPI was used for nuclear counterstaining, and image merging and analysis were performed using Fiji software (Fiji, USA).

Statistical analysis

All statistical analyses were performed using GraphPad Prism v8.0 (GraphPad Software Inc., USA). Data are presented as mean ± standard error. Comparisons between control and treated groups were made using an unpaired Student's t-test. A p-value of ≤ 0.05 was considered indicative of statistical significance. All experiments were repeated in triplicate to ensure data robustness, and results were analyzed to detect significant differences between the groups.

Acknowledgments

The authors would like to acknowledge Gujarat State Biotechnology Mission (GSBTM), Gujarat (GSBTM/JD(R&D)/618/21-22/00006135), and DBT-BUILDER Cat III (BT/INF/22/SP41403/2021) for financially supporting this research study. We sincerely appreciate the reviewers and editors for their insightful feedback, which has greatly contributed to improving the quality of our paper. L.P. is thankful to the Council for Scientific and Industrial Research (CSIR) - University Grants Commission (UGC), New Delhi, India, for their support in the form of a fellowship.

Conflicts of interest

The authors declare that no competing interests exist.

Author contributions

Lakshmi Pillai: Investigation, Data curation, Writing – original draft. Vishakha Nesari: Data curation. Dhanush Danes: Data curation. Suresh Balakrishnan: Conceptualization, methodology, Writing – review & editing.

References

ANTONUCCI R., ZAFFANELLO M., PUXEDDU E., PORCELLA A., CUZZOLIN L., DOLORES PILLONI M., FANOS V. (2012). Use of Non-steroidal Anti-inflammatory Drugs in Pregnancy: Impact on the Fetus and Newborn. *Current Drug Metabolism* 13: 474-490. https://doi.org/10.2174/138920012800166607

CHA Y. I., KIM S.H., SEPICH D., BUCHANAN F. G., SOLNICA-KREZEL L., DUBOIS R. N. (2006a). Cyclooxygenase-1-derived PGE 2 promotes cell motility via the G-protein-coupled EP4 receptor during vertebrate gastrulation. *Genes & Development* 20: 77-86. https://doi.org/10.1101/gad.1374506

CHA Y. I., KIM S.H., SOLNICA-KREZEL L., DUBOIS R. N. (2005). Cyclooxygenase-1 signaling is required for vascular tube formation during development. *Developmental Biology* 282: 274-283. https://doi.org/10.1016/j.ydbio.2005.03.014

CHA Y. I., SOLNICA-KREZEL L., DUBOIS R. N. (2006b). Fishing for prostanoids: Deciphering the developmental functions of cyclooxygenase-derived prostaglandins. *Developmental Biology* 289: 263-272. https://doi.org/10.1016/j.ydbio.2005.10.013

CHA Y. R., WEINSTEIN B. M. (2007). Visualization and experimental analysis of blood vessel formation using transgenic zebrafish. *Birth Defects Research Part C: Embryo Today: Reviews* 81: 286-296. https://doi.org/10.1002/bdrc.20103

CHÁVEZ M. N., AEDO G., FIERRO F. A., ALLENDE M. L., EGAÑA J. T. (2016). Zebrafish as an Emerging Model Organism to Study Angiogenesis in Development and Regeneration. *Frontiers in Physiology* 7: 56. https://doi.org/10.3389/fphys.2016.00056

CHILDS S., CHEN J.N., GARRITY D. M., FISHMAN M. C. (2002). Patterning of angiogenesis in the zebrafish embryo. *Development* 129: 973-982. https://doi.org/10.1242/dev.129.4.973

CHUNG A. S., LEE J., FERRARA N. (2010). Targeting the tumour vasculature: insights from physiological angiogenesis. *Nature Reviews Cancer* 10: 505-514. https://doi.org/10.1038/nrc2868

DANES D., RAVAL P., SINGH A., PILLAI L., BALAKRISHNAN S. (2024). Exposure to a sublethal dose of technical grade flubendiamide hampers angiogenesis in the chicken chorioallantoic membrane. *Toxicological Research* 40: 627-638. https://doi.org/10.1007/s43188-024-00254-z

ECKENSTALER R., RIPPERGER A., HAUKE M., PETERMANN M., HEMKEMEYER S. A., SCHWEDHELM E., ERGÜN S., FRYE M., WERZ O., KOEBERLE A., BRAUN H., BENNDORF R. A. (2022). A Thromboxane A 2 Receptor-Driven COX-2–Dependent Feedback Loop That Affects Endothelial Homeostasis and Angiogenesis. *Arteriosclerosis, Thrombosis, and Vascular Biology* 42: 444-461. https://doi.org/10.1161/ATVBAHA.121.317380

GORE A. V., MONZO K., CHA Y. R., PAN W., WEINSTEIN B. M. (2012). Vascular Development in the Zebrafish. *Cold Spring Harbor Perspectives in Medicine* 2: a006684-a006684. https://doi.org/10.1101/cshperspect.a006684

GROSSER T., YUSUFF S., CHESKIS E., PACK M. A., FITZGERALD G. A. (2002). Developmental expression of functional cyclooxygenases in zebrafish. *Proceedings of the National Academy of Sciences* 99: 8418-8423. https://doi.org/10.1073/pnas.112217799

HEIDEMAN W., ANTKIEWICZ D. S., CARNEY S. A., PETERSON R. E. (2005). Zebrafish and Cardiac Toxicology. *Cardiovascular Toxicology* 5: 203-214. https://doi.org/10.1385/CT:5:2:203

ISOGAI S., HORIGUCHI M., WEINSTEIN B. M. (2001). The Vascular Anatomy of the Developing Zebrafish: An Atlas of Embryonic and Early Larval Development. *Developmental Biology* 230: 278-301. https://doi.org/10.1006/dbio.2000.9995

IWASAKI R., TSUGE K., KISHIMOTO K., HAYASHI Y., IWAANA T., HOHJOH H., INAZUMI T., KAWAHARA A., TSUCHIYA S., SUGIMOTO Y. (2019). Essential role of prostaglandin E2 and the EP3 receptor in lymphatic vessel development during zebrafish embryogenesis. *Scientific Reports* 9: 7650. https://doi.org/10.1038/s41598-019-44095-5

KARAR J., MAITY A. (2011). PI3K/AKT/mTOR Pathway in Angiogenesis. *Frontiers in Molecular Neuroscience* 4: 51. https://doi.org/10.3389/fnmol.2011.00051

KAZENWADEL J., HARVEY N. L. (2016). Morphogenesis of the lymphatic vasculature: A focus on new progenitors and cellular mechanisms important for constructing lymphatic vessels. *Developmental Dynamics* 245: 209-219. https://doi.org/10.1002/dvdy.24313

LAMMERT E., AXNICK J. (2012). Vascular Lumen Formation. *Cold Spring Harbor Perspectives in Medicine* 2: a006619-a006619. https://doi.org/10.1101/cshperspect.a006619

LI W., JIN D., ZHONG T. P. (2019). Photoreceptor cell development requires prostaglandin signaling in the zebrafish retina. *Biochemical and Biophysical Research Communications* 510: 230-235. https://doi.org/10.1016/j.bbrc.2019.01.073

LIANG D., CHANG J. R., CHIN A. J., SMITH A., KELLY C., WEINBERG E. S., GE R. (2001). The role of vascular endothelial growth factor (VEGF) in vasculogenesis, angiogenesis, and hematopoiesis in zebrafish development. *Mechanisms of Development* 108: 29-43. https://doi.org/10.1016/S0925-4773(01)00468-3

LIVAK K. J., SCHMITTGEN T. D. (2001). Analysis of Relative Gene Expression Data Using Real-Time Quantitative PCR and the 2−ΔΔCT Method. *Methods* 25: 402-408. https://doi.org/10.1006/meth.2001.1262

MARTINA S. D., VESTA K. S., RIPLEY T. L. (2005). Etoricoxib: A Highly Selective COX-2 Inhibitor. *Annals of Pharmacotherapy* 39: 854-862. https://doi.org/10.1345/aph.1E543

MEYERS J. R. (2018). Zebrafish: Development of a Vertebrate Model Organism. *Current Protocols* 28: e19. https://doi.org/10.1002/cpet.19

NAKASHIMA F., GIMÉNEZ-BASTIDA J. A., LUIS P. B., PRESLEY S. H., BOER R. E., CHIUSA M., SHIBATA T., SULIKOWSKI G. A., POZZI A., SCHNEIDER C. (2023). The 5-lipoxygenase/cyclooxygenase-2 cross-over metabolite, hemiketal E2, enhances VEGFR2 activation and promotes angiogenesis. *Journal of Biological Chemistry* 299: 103050. https://doi.org/10.1016/j.jbc.2023.103050

NASEVICIUS A., LARSON J., EKKER S. C. (2000). Distinct Requirements for Zebrafish Angiogenesis Revealed by a VEGF-A Morphant. *Yeast* 1: 294-301. https://doi.org/10.1002/1097-0061(200012)17:4<294::AID-YEA54>3.0.CO;2-5

OTROCK Z., MAHFOUZ R., MAKAREM J., SHAMSEDDINE A. (2007). Understanding the biology of angiogenesis: Review of the most important molecular mechanisms. *Blood Cells, Molecules, and Diseases* 39: 212-220. https://doi.org/10.1016/j.bcmd.2007.04.001

PAKRASI P. L., JAIN A. K. (2007). Evaluation of cyclooxygenase 2 derived endogenous prostacyclin in mouse preimplantation embryo development in vitro. *Life Sciences* 80: 1503-1507. https://doi.org/10.1016/j.lfs.2007.01.044

PARMAR B. K., VERMA U. R., VAISHNAV J. A., BALAKRISHNAN S. (2022). Cyclooxygenase-2 plays a crucial role during myocardial patterning of developing chick. *The International Journal of Developmental Biology* 66: 373-381. https://doi.org/10.1387/ijdb.220153sb

PARMAR B., VERMA U., KHAIRE K., DANES D., BALAKRISHNAN S. (2021). Inhibition of Cyclooxygenase-2 Alters Craniofacial Patterning during Early Embryonic Development of Chick. *Journal of Developmental Biology* 9: 16. https://doi.org/10.3390/jdb9020016

PILLAI L., KARANDIKAR S., PANDYA K., V.M. A., SINGH A., BALAKRISHNAN S. (2024). Exposure to thiourea during the early stages of development impedes the formation of the swim bladder in zebrafish larvae. *Journal of Applied Toxicology* 44: 1572-1582. https://doi.org/10.1002/jat.4657

PINI B., GROSSER T., LAWSON J. A., PRICE T. S., PACK M. A., FITZGERALD G. A. (2005). Prostaglandin E Synthases in Zebrafish. *Arteriosclerosis, Thrombosis, and Vascular Biology* 25: 315-320. https://doi.org/10.1161/01.ATV.0000152355.97808.10

RIBATTI D., CRIVELLATO E. (2012). "Sprouting angiogenesis", a reappraisal. *Developmental Biology* 372: 157-165. https://doi.org/10.1016/j.ydbio.2012.09.018

RICCIOTTI E., FITZGERALD G. A. (2011). Prostaglandins and Inflammation. *Arteriosclerosis, Thrombosis, and Vascular Biology* 31: 986-1000. https://doi.org/10.1161/ATVBAHA.110.207449

SCHUERMANN A., HELKER C. S. M., HERZOG W. (2014). Angiogenesis in zebrafish. *Seminars in Cell & Developmental Biology* 31: 106-114. https://doi.org/10.1016/j.semcdb.2014.04.037

TAKAHASHI Y., KITADAI Y., BUCANA C. D., CLEARY K. R., ELLIS L. M. (1995). Expression of vascular endothelial growth factor and its receptor, KDR, correlates with vascularity, metastasis, and proliferation of human colon cancer. *Cancer Research* 55: 3964-3968.

UDAN R. S., CULVER J. C., DICKINSON M. E. (2013). Understanding vascular development. *WIREs Developmental Biology* 2: 327-346. https://doi.org/10.1002/wdev.91

UGWUAGBO K. C., MAITI S., OMAR A., HUNTER S., NAULT B., NORTHAM C., MAJUMDER M. (2019). Prostaglandin E2 promotes embryonic vascular development and maturation in zebrafish. *Biology Open* 8: bio039768. https://doi.org/10.1242/bio.039768

VERMA U., GAUTAM M., PARMAR B., KHAIRE K., WISHART D. S., BALAKRISHNAN S. (2021). New insights into the obligatory nature of cyclooxygenase-2 and PGE2 during early chick embryogenesis. *Biochimica et Biophysica Acta. Molecular and Cell Biology of Lipids* 1866: 158889. https://doi.org/10.1016/j.bbalip.2021.158889

WIENS K. M., LEE H. L., SHIMADA H., METCALF A. E., CHAO M. Y., LIEN C.L. (2010). Platelet-Derived Growth Factor Receptor β Is Critical for Zebrafish Intersegmental Vessel Formation. *PLoS ONE* 5: e11324. https://doi.org/10.1371/journal.pone.0011324

XU D., BU J., GU S., XIA Y., DU J., WANG Y. (2011). Celecoxib Impairs Heart Development via Inhibiting Cyclooxygenase-2 Activity in Zebrafish Embryos. *Anesthesiology* 114: 391-400. https://doi.org/10.1097/ALN.0b013e3182039f22